Short Communication

Influence of Molybdenum as Alloying Element on Corrosion Resistance of Stainless Steel Rebar in Simulated Concrete Pore Solution with different pH

Jitao Fan[1], Qizhi Zhang[2]*

[1] Zhumadian Construction Company, Zhumadian, 463000, China
[2] Huanghuai University, Zhumadian, 463000, China
*E-mail: fanjitao111@163.com, 20070359@huanghuai.edu.cn,

Reinforcement stainless steel working electrode was successfully used in electrochemical testing after 5 h immersion in simulated concrete pore (SCP) solutions. The influence of molybdenum (Mo) element addition into the alloy steel on the corrosion behavior of steel rebar in different pH value of SCP solutions was evaluated using Mott–Schottky and electrochemical impedance spectroscopy (EIS) analysis. Results showed that pH value of SCP solution had a significant effect on the formation of the passive layer on reinforcement steel. The EIS results indicated that the increase of Mo content improves the passive layer stability, boosts the polarization resistance and enhances the corrosion resistance of the steel rebar. Furthermore, the value of the double-layer capacitance decreased as pH and Mo content reduced, which revealed that the passive film thickness increased and the resulting protective capacity enhanced when the pH and Mo content of reinforced concrete was gradually increased. The minimum values of donor density were obtained for a Mo concentration of 3 wt% and 12 pH value of solution which are in good agreement with the experimental results.

1. INTRODUCTION

Reinforced concretes are the most widely used materials in the construction because of their durable and economical properties [1]. The embedded steel rebar in concrete structures not only helps to make the structure with the highest compressive strength but also assists to create a protective environment for the rebar [2]. Several methods have been tried to protect the concrete from corroding in highly corrosive surroundings like galvanized rebar, epoxy coated rebar and the addition of inhibitors in the concrete mix [3]. However, there is still a need for a more protective solution because

all these methods have drawbacks. The durability of reinforced concrete structures in a corrosive environment can be guaranteed by stainless steel [4]. Recently, stainless steel has become a more acceptable rebar compared to the conventional austenitic ones because of its high corrosion resistance in concrete [5, 6]. The protective layer is enhanced by the alloying elements used in the steel, making it more suitable for environment containing chloride ions [7]. Many studies were performed to optimize the composition of steel in the enhancement of the structure industry. Liu et al. [8] exhibited the influence of pH value and chromium on the formation of passive layer of steel rebars which leeds to the highest corrosion resistance. Wang et al. [9] showed the hydroxyl carbon nanotubes and polyvinyl alcohol as modifiers can improve the corrosion resistance of steel rebars in concrete. Ha et al. [10] investigated the molybdenum contribution in pitting corrosion resistance of rebar and its reinforcement mechanism. Although there are many reports on the alloying elements used in the steel to improve the corrosion resistance of stainless steel have been published, very little research have been reported for the effect of Mo content on corrosion behavior of steel rebar. In this study the passivation and corrosion-resistant of steel rebar in basic solutions with various pH values were considered. Electrochemical impedance spectroscopy and Mott-Schottky theory were used to examine the effect of molybdenum addition on the electrochemical properties of steel bars in the simulated concrete pore solution.

2. MATERIALS AND METHOD

In this study, stainless steel rebars with 6 mm diameter and 10 mm length were utilized to study the effect of Molybdenum (Mo) content and pH of solution on electrochemical corrosion behavior. Table 1 indicates the chemical composition of stainless steel rebars used in the present work.

Table 1. Chemical composition (wt.%) of the steel rebars

Alloys	C	Si	Mn	P	S	Cr	Mo	Fe
0 Mo	0.12	0.6	1.0	0.04	0.03	12.5	-	Balance
1 Mo	0.12	1.0	1.0	0.04	0.03	16	1.0	Balance
2 Mo	0.1	0.8	1.3	0.04	0.03	16	2.0	Balance
3 Mo	0.1	0.8	1.0	0.04	0.03	16	3.0	Balance

The specimens were polished with SiC sheets, and then ultrasonically washed in acetone solution and rinsed in deionized water. The electrical contact was attained using a copper wire attached to the end of reinforcement steel samples.

The simulated concrete pore (SCP) solution was prepared using 5 g L^{-1} of KOH, 0.75 g L^{-1} NaOH, and 0.75 g L^{-1} Ca(OH)$_2$. The mass fraction of NaCl in the solution was 1.0%. The pH of solutions was adjusted by adding a varying amount of NaHCO$_3$ in 10.0, 11.0, 12.0 and calibrating by a pH meter (Sigma, P1367 MSDS). A three-electrode system, including the steel rebar as a working electrode, graphite as a counter electrode and saturated calomel electrode as a reference electrode was

used. The electrochemical analysis of the samples was performed after immersion time of 5 houres. EIS (CorrTest Instruments Corp., Ltd., China) tests were conducted at open circuit potential with a scanning range of 10 mHz to 100 kHz at the amplitude of 10 mV. ZSimpWin was used to interpret the experimental results. Mott-Schottky was carried out from -1.0 V to 1.0 V at a rate of 50 mv/s, and the measured frequency was 1 kHz. All the tests were carried out at room temperature. The morphologies of the samples corroded in the SCP solution for 5 h were examined using scanning electron microscope (SEM, FEI/Nova NanoSEM 450).

3. RESULTS AND DISCUSSION

EIS technique has been extensively employed in the analysis of the passive layer of rebars due to its capability to characterize redox reactions of steel rebars in an alkaline environment.
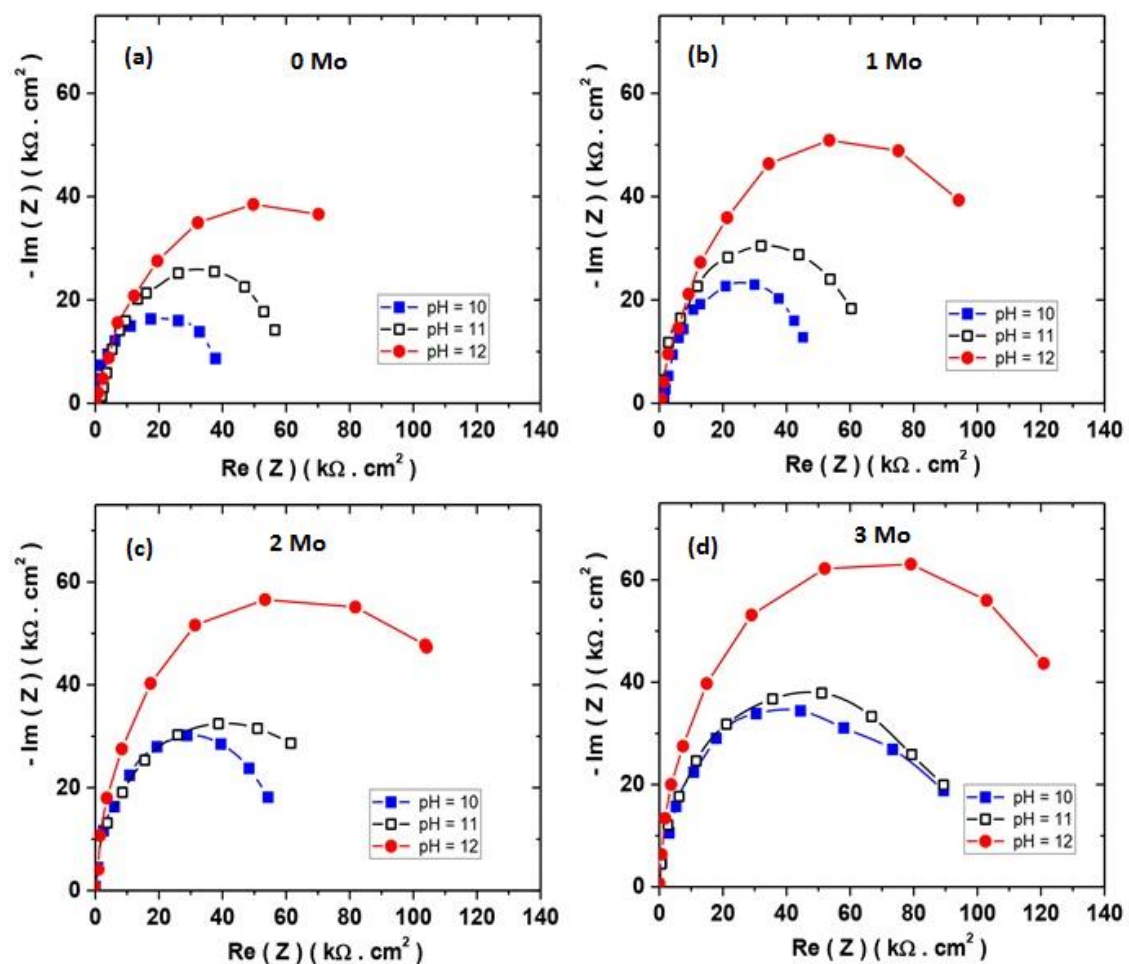

Figure 1. Nyquist plots obtained from stainless steels with different Mo content in the simulated concrete pore solution at different pH value

EIS was conducted to analyze the pH effect on the corrosion behavior of rebars with passive layers in simulated concrete pore solution. As shown in figure 1, the increase in pH value leads to an

increase in the radius of the capacitive loop which indicates enhancement of the corrosion resistance for reinforced concrete. Furtheremore, at a constant pH, the increase in Mo content reduced the radius of the capacitive loop implying the enhancement of corrosion resistance by molybdenum addition. It can be attributed to the formation of a protective passive layer.

　　　　Figure 2 indicates an equivalent circuit used to model the impedance spectra. Rs is the solution resistance. R_f and R_{ct} are the resistance of passive film and the charge-transfer resistance, respectively. CPE_f and CPE_{dl} are the passive film/solution interface capacitance and double-layer capacitance [11].
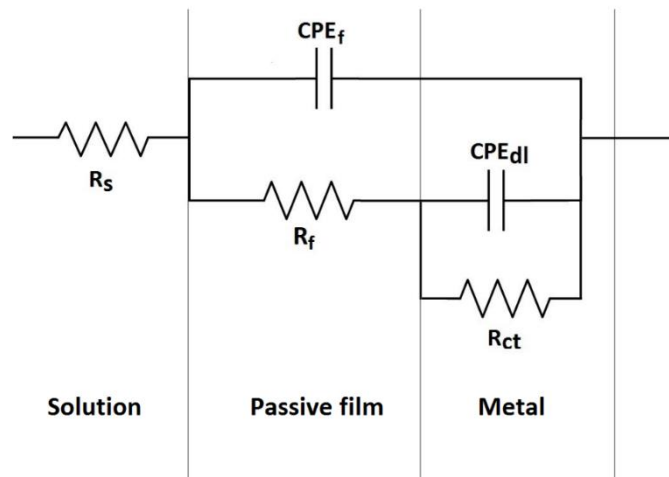

Figure 2. An equivalent circuit model to fit the experimental data

Table 2. Electrochemical parameters from the fitting using the equivalent circuit in Figure 2 for different pH values of solution and various content of Mo

Alloys	pH	R_s (Ω cm²)	R_f (kΩ cm²)	CPE_f (μF cm⁻²)	R_{ct} (kΩ cm²)	CPE_{dl} (μF cm⁻²)
0 Mo	10	26.2	20.8	16.7	40.3	17.6
	11	44.6	33.6	6.9	62.8	8.4
	12	67.8	49.5	3.6	93.2	4.3
1 Mo	10	32.4	32.3	14.6	46.7	14.8
	11	65.7	46.4	4.8	72.6	6.5
	12	71.2	61.2	3.1	115.2	3.6
2 Mo	10	28.9	35.1	7.5	63.5	8.7
	11	63.5	58.4	3.5	91.6	4.8
	12	69.3	72.9	2.9	137.8	3.2
3 Mo	10	32.6	56.3	3.8	94.6	4.1
	11	68.2	73.6	3.2	112.3	3.5
	12	75.6	76.8	2.5	162.9	2.8

　　　　Polarization resistance, R_p ($R_p = R_f + R_{ct}$) is a computable indicator to consider the steel corrosion resistance in the corrosive environment. So that the higher Rp value indicates higher corrosion resistance of the sample.

According to table 2, increasing the pH values in solution and Mo contents of alloys show an sinificantly enhancement in Rp value indicating a higher corrosion resistance for 3 Mo rebar in pH 12.

The thickness of the passive film can be determined with the following equation [12]:

$$D = \frac{\varepsilon\varepsilon_0 A}{Q} \qquad (1)$$

Where D is the thickness of the passive film, ε_0 (8.85×10^{-12} F m^{-1}) and ε (12 for Fe oxides) are the vacuum permittivity and dielectric constant, respectively. A and Q are an effective area and capacitance, respectively.

As shown in table 2, the value of CPE$_{dl}$ (Q) decreased as pH and Mo content reduced, which reveals that the passive film thickness increased and the resulting protective capacity enhanced when the pH and Mo content of reinforced concrete gradually increased. In constant pH value, the R$_f$ passive film resistance increased as the Mo content in alloy increased, which indicates that the protective feature of the passive film developed is strong. Compared to CPE$_f$ and CPE$_{dl}$, it was found that CPE$_f$ is lower than CPE$_{dl}$ which confirm the formation of thin passive film and the double layer at the interfaces has a high capacitive behavior.
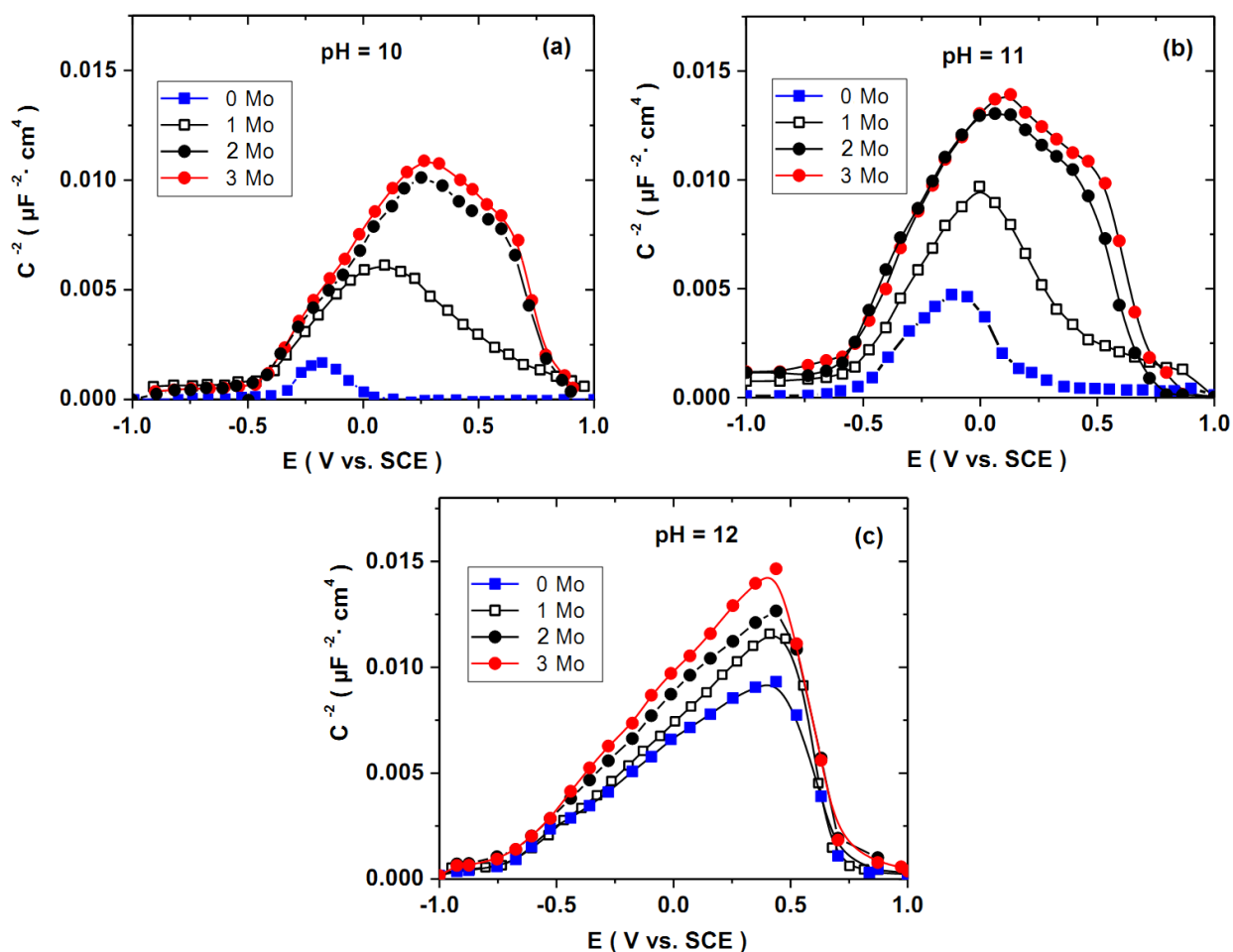

Figure 3. Mott-Schottky plots of stainless steels with different Mo content in the simulated concrete pore solution at pH of (a) 10 (b) 11 and (c) 12.

The charge distributions at the interface between an electrolyte and a semiconductor was determined by calculating the interfacial capacitance as a function of the electrode potential (E). When the space charge double layer (C_{sc}) assists as a depletion layer, the relationship between the capacitance and the potential can be evaluated by the Mott-Schottky equation [13]:

$$\frac{1}{C_{sc}^2} = \frac{2}{\varepsilon \varepsilon_0 e N_d}\left(E - E_{fb} - \frac{kT}{e}\right) \qquad (2)$$

where e is electron charge (1.602×10^{19} C). N and E_{fb} are donor densities and flat-band potential, respectively. k and T are Boltzmann's constant (1.38×10^{23} J/K) and thermodynamic temperature, respectively. kT/e is approximately 25 mV at the ambient temperature. N_d is a density of point defect. N_d can be gained based on the slope of the experimental C_{sc}^{-2} vs E diagrams. E_{fb} can be calculated according to the slope and intercept.

Figure 3 shows the effect of various pH values and Mo contents on the Mott-Schottky plots of stainless steel rebar immersed in SCP solutions. Negative slope of the Mott-Schottky plots for all the specimens was observed in the high potential range and positive one was appeared at the low potential. When the slope is positive, it shows that the passive film on the sample exposed to various solutions is an n-type semiconductor [14, 15]. As shown in the figure 3, the linear regions appeared in all curves, Related to the potential values from - 0.4 V to 0.3 V.

The values of N_d are listed in figure 4. As shown, by adding a small amount of Mo in alloy, the donor density significantly reduced. The minimum values were obtained for a Mo concentration of 3 wt% and 12 pH of solution. These are consistent with the experimental results described above. The orders of magnitude in donor density was 10^{20} which was in good agreement with values reported in the literature [16].
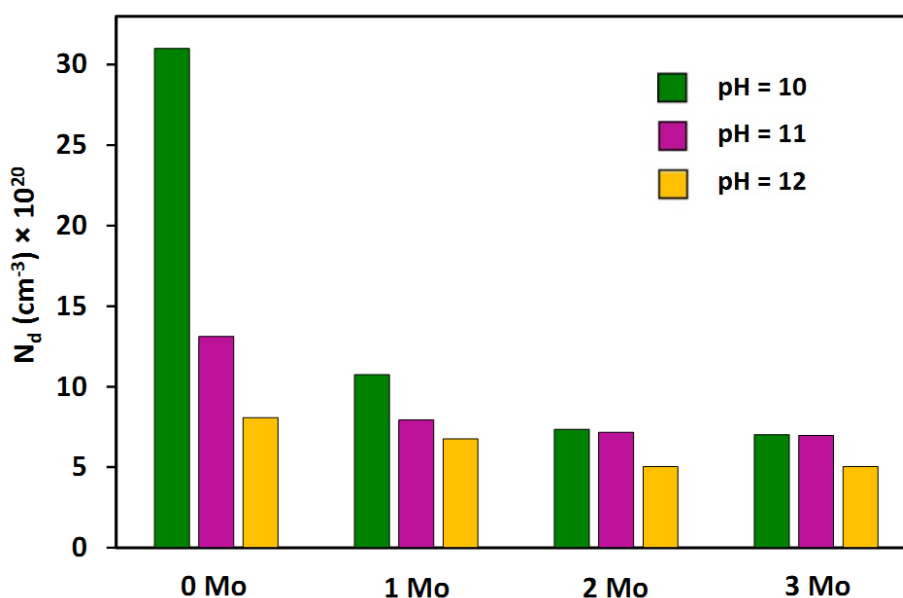

Figure 4. N_d values of stainless steels with different Mo content in the simulated concrete pore solution at various pH.

Chloride (Cl⁻) ions are known as erosion ions for reinforcement steel, and the basic mechanisms of corrosion in the passive layer have been widely studied. Consistent with the point defect model [17], the formation of passive film on the reinforcement steel surface had a spinel structure with several defects in tetrahedral and octahedral space [18] and other regions, for example grain boundary, dislocation, second phase, and other discontinuous areas. All of these landscapes result in the penetration of anions or cations into the passive layer and subsequently lead to the dissolution of iron. Thus, Cl⁻ ions can influence in the passive film defects, and constantly destroy the passive layer by local acidification and self-catalysis effect. The participation of Cl⁻ ions in the passive film formation lead to a decrease in compactness of the corrosion product layer.

With increasing Mo content, the value of E where the discontinuous changes occur increases. This indicates an increase concentrations of Fe^{3+} and MoO_2, a decrease in concentration of oxygen holes, and a relatively improved corrosion resistance by the corrosion product layer. The minimum N_d value were observed for a 3 Mo alloy at pH of 12. These are in good agreement with the experimental results described above.
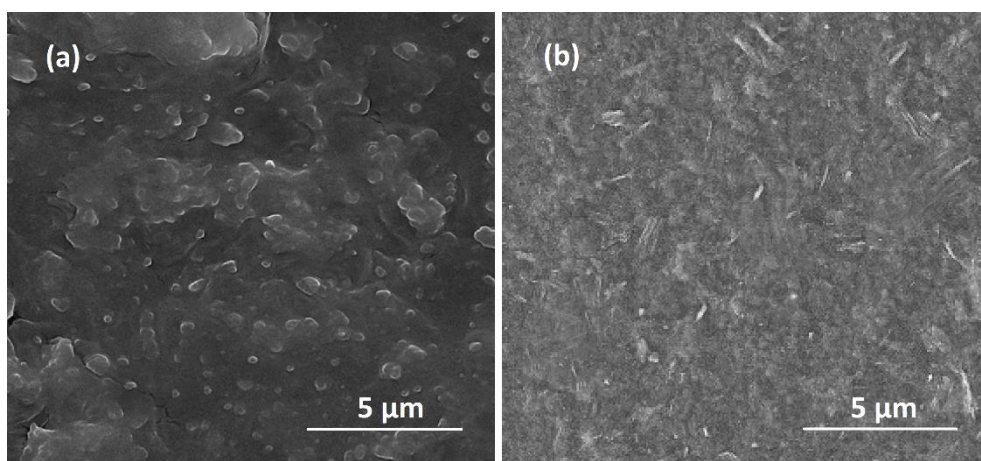

Figure 5. SEM images of stainless steel surfaces with (a) 0 wt% Mo and (b) 3 wt% Mo after immersion in SCP solution at pH of 12

Figure 5 shows the SEM images of 0 Mo and 3 Mo stainless steel after immersion in SCP solution at pH of 12. In SCP solution at pH of 12, the surface of 0 Mo alloy has a lot of corrosion products and pits, showing that severe pitting corrosion occurred on the surface of steel rebar (Fig. 5a), which is consistent with the results extracted from EIS Mott-Schottky plots. As shown in figure 5b, with the increase of Mo element content, steel corrosion degree decreased significantly. The results of SEM confirmed that increase of Mo content in the alloys could stop the growth of micro-pits and thus prolong the period of pitting corrosion.

4. CONCLUSIONS

This paper mainly studied the corrosion resistance of the Mo addition in alloy steels exposed to various pH values in SCP solutions. EIS and Mott-Schottky analysis were used to examine the samples. The EIS results indicate that the addition of Mo element enhanced the passive layer of steel immersed in the SCP solution. At a constant pH, an increase in Mo content increased the range of passivation and pitting potential and improved polarization resistance, indicating the enhancement of corrosion resistance. The value of double-layer capacitance decreased as pH and Mo content reduced, which reveals that the passive film thickness increased and the resulting protective capacity enhanced when the pH and Mo content of reinforced concrete gradually increased. The SEM images of the surface of stainless steel confirmed that increasing the Mo content in the alloys could stop the growth of micro-pits and thus prolong the period of pitting corrosion.

References

1. N. Xue, X. Liu, H. Jia, Y. Wu and J. Ma, *International Journal of Electrochemical Science*, 11 (2016) 8430.
2. X. Wang, Y. Liu, F. Yang, Y. Lu and X. Li, *Construction and Building Materials*, 229 (2019) 116855.
3. H. Chen, S. Zhang, Z. Zhao, M. Liu and Q. Zhang, *Progress in Chemistry*, 31 (2019) 571.
4. D. Yuan, C. Zhang, S. Tang, X. Li, J. Tang, Y. Rao, Z. Wang and Q. Zhang, *Water research*, 163 (2019) 114861.
5. C. Monticelli, M. Criado, S. Fajardo, J. Bastidas, M. Abbottoni and A. Balbo, *Cement and concrete research*, 55 (2014) 49.
6. S. Tang, N. Li, D. Yuan, J. Tang, X. Li, C. Zhang and Y. Rao, *Chemosphere*, 234 (2019) 658.
7. F. Husairi, J. Rouhi, K. Eswar, A. Zainurul, M. Rusop and S. Abdullah, *Applied Physics A*, 116 (2014) 2119.
8. M. Liu, X. Cheng, X. Li, C. Zhou and H. Tan, *Construction and Building Materials*, 130 (2017) 193.
9. P. Shao, J. Tian, F. Yang, X. Duan, S. Gao, W. Shi, X. Luo, F. Cui, S. Luo and S. Wang, *Advanced Functional Materials*, 28 (2018) 1705295.
10. J. Rouhi, C.R. Ooi, S. Mahmud and M.R. Mahmood, *Materials Letters*, 147 (2015) 34.
11. H. Luo, C. Dong, X. Li and K. Xiao, *Electrochimica Acta*, 64 (2012) 211.
12. P. Shao, J. Tian, X. Duan, Y. Yang, W. Shi, X. Luo, F. Cui, S. Luo and S. Wang, *Chemical Engineering Journal*, 359 (2019) 79.
13. B. Lin and Y. Xu, *International Journal of Electrochemical Science*, 14 (2019) 75.
14. X. He, F. Deng, T. Shen, L. Yang, D. Chen, J. Luo, X. Luo, X. Min and F. Wang, *Journal of colloid and interface science*, 539 (2019) 223.
15. P. Xu, L. Jiang, M.-Z. Guo, J. Zha, L. Chen, C. Chen and N. Xu, *Construction and Building Materials*, 223 (2019) 352.

16.   M. Husairi, J. Rouhi, K. Alvin, Z. Atikah, M. Rusop and S. Abdullah, *Semiconductor Science and Technology*, 29 (2014) 075015.
17.   B. Krishnamurthy, R.E. White and H.J. Ploehn, *Electrochimica acta*, 47 (2002) 3375.
18.   S.A. El Haleem, S.A. El Wanees and A. Bahgat, *Corrosion Science*, 87 (2014) 321.